Int. J. Heat Mass Transfer. Vol. 34, No. 1, pp. 217–227, 1991
Printed in Great Britain

0017–9310/91 $3.00 + 0.00

Computation of macrosegregation in an iron–carbon cast

GUSTAV AMBERG
Department of Hydromechanics, Royal Institute of Technology, S-100 44 Stockholm, Sweden

(*Received* 16 *October* 1989)

Abstract—A numerical method for computation of macrosegregation in a solidifying alloy is presented. The formulation relies only on the fundamental conservation laws for mass, momentum, heat and solute, and the thermodynamical relations governing phase change. The entire time-dependent process is simulated, up to complete solidification. The method is applied to the case of an iron–carbon system solidifying in a two-dimensional rectangular mould, cooled from the sides. The thermal and solutal convection that arises during solidification is computed. The evolution of the melt fraction in the mould, and the final distribution of carbon after solidification, is reported.

1. INTRODUCTION

DURING solidification of alloys, it is well known that a so-called mush, a two-phase region containing both solid and liquid metal, often forms on the cooled wall, instead of a plane solidification front. It has long been realized [1], that macroscopic convection through the mush during solidification is the primary cause of macrosegregation. When a melt is poured into a mould and cooled from the sides a strong thermal convection is immediately set up in the completely molten region. Another mechanism is that the melt in the mush is often enriched in solute as the solidification proceeds, and this may then cause a macroscopic solutal convection through the mush. Both of these convective motions will be active in redistributing the solute and thus in producing macrosegregation.

This paper presents a numerical computation of the time-dependent solidification of an alloy, with the aim of simulating the entire process to gain a better understanding of macrosegregation. The solidification of an iron–carbon system is presented. The melt is cooled from the sides, and the top and bottom are insulated. The process is followed to complete solidification so that the resulting macrosegregation is obtained.

If convective and diffusive transport of solute through the mush is negligible, the evolution of the composition of the melt and the solid is easily obtained from either Scheil's equation or the so-called lever rule [2]. An important early study of macrosegregation is that by Flemings and Nereo [1], who studied the slow convection induced by solidification shrinkage and computed the corrections to the Scheil equation and the lever rule.

Many numerical computations of a solidifying alloy have been presented in the literature, such as Voller and Prakash [3], and Flood and Hunt [4]. However, in the vast majority of these reports, an algebraic relation between temperature and melt fraction in the spirit of a Scheil equation or a lever rule is utilized. Such a relation is strictly true only when macroscopic transport of solute is negligible. Such computations may thus predict the evolution of melt fraction and temperature during solidification, but will not give any information about the distribution of solute in the solidified ingot.

Hills *et al.* [5] presented a fairly complete set of equations allowing diffusive and convective transport of solute and heat. Using such a formulation, Worster [6] managed to obtain very instructive semi-analytic solutions to the problem of solidification with mass diffusion but without convection.

Bennon and Incropera [7], and Beckermann and Viskanta [8], using the same numerical method, solved for composition and temperature separately and were able to predict a true macrosegregation. Their numerical technique is somewhat different from that presented here, the relative merits of the two approaches will be discussed below. Also we have computed solidification of metals, while they computed solidification of various salts with which they also made experiments.

This paper is planned as follows: the mathematical problem is formulated in Section 2, then the numerics are discussed briefly in Section 3. The solidification of an iron–carbon system has been computed and the results are presented and discussed in Section 4. Section 5 contains concluding remarks.

2. FORMULATION

In this section the mathematical problem to be solved is formulated. In this we follow Hills *et al.* [5]. The solidification process is governed by the balance of momentum and the conservation of heat, solute and total mass. The primary unknowns are: $\mathbf{u}$, p the mean melt velocity and pressure; T the temperature;

NOMENCLATURE

a	half width
b	height
C	specific heat
c	composition
Co	Courant number
D	mass diffusivity
d	coefficient in equation (2)
e	parameter in equation (2)
f	solutal expansion coefficient
$H(\chi)$	permeability
k	average heat conductivity in mush
k_p	partition ratio, c_s/c_l
L	latent heat of fusion
p	pressure
Pr	Prandtl number
Q	prescribed heat flux at the side walls
Ra	Rayleigh number
T	temperature
T_0	melting temperature of pure iron
$T_L(c_l)$	liquidus temperature
$\mathbf{u}$	mean melt velocity
Y_1, Y_2	parameters in equation (3).

Greek symbols

α'	thermal expansion coefficient
Γ	slope of liquidus line
ε	numerical parameter in equation (14)
μ	viscosity
ρ	density
χ	fraction of volume occupied by melt.

Subscripts

0	reference quantity
i	initial values
l	liquid-phase quantity
m	mixture quantity
s	solid-phase quantity.

c_l, c_s, c_m the composition of liquid, solid and mixture, respectively; χ the fraction of volume occupied by melt.

We consider a two-dimensional rectangular mould with width $2a$ and height b. The side walls are cooled, and the top and bottom are insulated. The centreline $x = a$ is a line of symmetry so that only the domain $0 < x < a$, $0 < y < b$ needs to be computed. A frame of reference with horizontal coordinate x and vertical coordinate y, opposite to gravity, will be used as shown in Fig. 1.

During the solidification three regions are distinguishable in the mould, containing solid, mush and liquid metal, respectively. The balance of linear momentum, as well as all other equations, is expressed as an equation which is valid in all three regions, so that no explicit tracking of the front of the mushy zone is necessary.

Expressed in the fluid velocity, the balance of linear momentum takes the following form:

$$\rho_0\left(\frac{\partial \mathbf{u}}{\partial t}+\mathbf{u}\cdot\nabla\mathbf{u}\right)-\mu\Delta\mathbf{u} = -\nabla p - \rho g \mathbf{e}_y - \frac{\mu}{H(\chi)}\chi\mathbf{u} \tag{1}$$

where $\mathbf{u} = (u, v)$ denotes the fluid velocity (m s^{-1}). In the mush it is to be interpreted as an average over the pore spaces. p is the pressure (N m^{-2}), T the temperature (°C), c_l the weight fraction of solute in the melt. The fluid viscosity is denoted by μ (kg m^{-1} s^{-1}), and ρ_0 (kg m^{-3}) is a reference density taken as the initial density of the melt. g is the gravitational acceleration (9.81 m s^{-2}).

The melt density ρ depends on temperature T and composition c_l. Correlations for the iron–carbon system have been given by Olsson [9]

$$\rho = \rho_0(1+\alpha'(T-1536°\text{C})+f\cdot c_l)$$

where

$$\alpha' = \frac{d}{e+100\cdot c_l}. \tag{2}$$

Values of the parameters d, e, f are given in Table 1.

The size of the dendrites is small, typically 0.1 mm, so that the mush may be treated as a porous medium. $H(\chi)$ (m^2) is the permeability of the mush, defined as is common in the theory of porous media. The permeability is a function of the volume fraction melt (or porosity) χ. It may be estimated crudely as the square of a typical dendrite spacing. In this paper we use a correlation for the function $H(\chi)$, appropriate for a metal mush, which has been given by West [10]:

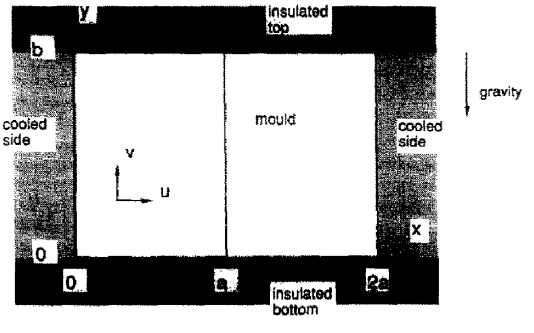

FIG. 1. The geometry of the mould.

Table 1. Physical properties of an iron–carbon alloy

μ	viscosity	6.94×10^{-3} N s m^{-2}
ρ_0	density	6940 kg m^{-3}
C	specific heat	753 J kg^{-1} °C^{-1}
L	latent heat of fusion	2.72×10^{5} J kg^{-1}
k_l	heat conductivity in liquid	30 W m^{-1} °C^{-1}
k_s	heat conductivity in solid	60 W m^{-1} °C^{-1}
D	mass diffusivity	1×10^{-9} m^2 s^{-1}
T_0	melting temperature of pure iron	1536°C
Γ	slope of liquidus line	7800°C (wt frac)$^{-1}$
k_p	partition ratio	0.42
d	coefficient in equation (2)	-4.2×10^{-4}
e	parameter in equation (2)	0.55
f	solutal expansion coefficient	−8
Y_1	parameter in equation (3)	6.4×10^{-13} m^2
Y_2	parameter in equation (3)	8.8×10^{-11} m^2

$$H(\chi) = Y_1 \cdot K_1 + Y_2 \cdot K_2,$$

where

$$K_1 = \chi^2$$

$$K_2 = 0 \text{ if } \chi < 1/3$$

$$K_2 = (1-\chi)^{2/3}\left(3+\frac{4}{1-\chi}-3\sqrt{\left(\frac{8}{1-\chi}-3\right)}\right)$$

$$\text{if} \quad \chi > 1/3. \tag{3}$$

Values of Y_1 and Y_2 are given in Table 1. In the completely molten region where the volume fraction of melt χ is 1, $H(\chi)$ is infinite so that the last term on the right-hand side of equation (1) vanishes, leaving the usual Navier–Stokes equation for fluid flow. Whenever a mush appears, so that χ decreases below 1, $H(\chi)$ very rapidly decreases to very small values, typically less than 10^{-8} m^2. Then the velocities will be very much smaller and the terms on the left-hand side of equation (1) are negligible. The remaining terms on the right-hand side are in fact the Darcy law, known to hold in porous media. We have not included the dependencies of melt fraction χ in equation (1) that would make this equation valid for a mush so thin that the two left-hand side terms, representing inertia and macroscopic shear, are important. Since the permeability is very low this does not seem to occur, and so it is not a serious limitation to use the form given in equation (1).

In formulating equation (1) the standard Boussinesq approximation has been invoked, in assuming that density variations are important only in the buoyancy terms (the second term on the right-hand side).

The solid and liquid metal are assumed to be incompressible, and the solidification shrinkage is neglected, in accordance with the Boussinesq approximation used in the momentum equation. With this approximation the conservation of total mass reduces to

$$\nabla\cdot(\chi\mathbf{u}) = 0. \tag{4}$$

The time required for thermal diffusion over a pore size distance may be estimated and is found to be very short. Any temperature variation with a length scale of the same order of magnitude as a dendrite spacing is thus quickly smoothed out and so, in the mush, the temperature is essentially the same in both the liquid and solid phase. Thus the conservation of heat can be formulated in terms of an equation for a single temperature, valid throughout the liquid, mushy and solid regions

$$\rho_0 C\left(\frac{\partial T}{\partial t}+\chi\mathbf{u}\cdot\nabla T\right) = \nabla\cdot k\nabla T - \rho_0 L\frac{\partial\chi}{\partial t}. \tag{5}$$

Here C is the specific heat of the metal (J kg^{-1} °C^{-1}) and L the latent heat of fusion (J kg^{-1}). k (W m^{-1} °C^{-1}) is the heat conductivity, which is taken as an average of the heat conductivity in the solid and liquid phases: $k = \chi k_l + (1-\chi)k_s$, where k_l, k_s are heat conductivities in liquid and solid metal, respectively.

Conservation of solute is formulated in a way similar to equation (5). However, mass diffusion is much slower than heat diffusion, especially in the solid, so the composition of the solid in a dendrite arm is not necessarily in equilibrium with the composition of the interdendrite liquid. Two different approximations are commonly used: either the assumption of a rapid diffusion in the dendrites, so that the composition is always essentially uniform across a dendrite arm, or the opposite, no diffusion at all in the solid. The composition at the surface of the dendrite is then determined by the composition of the interdendrite liquid alone and is completely unaffected by the composition inside the dendrite. If macroscopic transport of solute is neglected, the former leads to the lever rule and the latter to the Scheil equation. In the iron–carbon system that is considered here, the appropriate approximation is that of rapid diffusion in the solid. In the liquid, the mass diffusivity is always assumed to be large enough, so that the composition is practically uniform over a dendrite spacing.

However, since the solubility of the solute is normally different in the solid and the liquid state it is necessary to work with the composition of the liquid

c_l, and the composition of the solid c_s separately. At a point in the mush these will then mean the almost constant values of the alloy content in the melt filling a dendrite spacing, or the solid in a dendrite arm, respectively. It will also be practical to introduce the net composition of the solid–liquid mixture

$$c_m = \chi c_l + (1-\chi)c_s. \tag{6}$$

Considering the conservation of mass of the solute the following equation is now easily obtained:

$$\frac{\partial c_m}{\partial t} + \nabla \cdot (\mathbf{u}\chi c_l) = \nabla \cdot D\nabla c_m. \tag{7}$$

Note that, in the absence of convection and diffusion, this equation merely states that c_m is constant, which is the so-called lever rule. It should also be pointed out that, even though mass diffusivity D is large enough to smooth out variations on the dendrite length scale, mass diffusion is still small compared to convective transport on the macroscopic scale. Consequently the precise form of the term on the right-hand side is not important.

The solidification of an alloy is to a large extent governed by the phase diagram, i.e. the relations between temperature and composition at phase boundaries. This may be quite complicated, with phase transitions between different crystal structures, etc. However, for the transition between solid and liquid in an iron–carbon system, the relation between temperature and composition of the melt (liquidus line) may be approximated as a linear function

$$T = T_L(c_l) = T_0 - \Gamma c_l \tag{8}$$

where T_0 is the melting temperature of the pure metal and the constant of proportionality Γ is in units of °C (wt frac)$^{-1}$.

The solubility of the solute is normally different in the solid and the liquid state so that c_l and c_s are related according to the partition ratio k_p

$$c_s = k_p c_l. \tag{9}$$

The relation between temperature and composition of the solid (solidus line) follows from equations (8) and (9), and has thus also been approximated to be linear.

Relations (8) and (9) must hold on interfaces where solid and liquid meet, i.e. on dendrite surfaces in the mush. Since temperature and composition variations are small over distances of the order of dendrite spacing, they must indeed hold throughout the mush.

Equations (1)–(9) must be supplemented by boundary conditions for $\mathbf{u}$, T and c_m. The centreline is a line of symmetry so only the left half of the mould is computed. All sides of the mould are assumed to be solid, so the appropriate boundary conditions for $\mathbf{u}$ are

$$\mathbf{u} = 0 \quad \text{at} \quad x = 0 \quad \text{and} \quad y = 0, b$$

$$u = \frac{\partial v}{\partial x} = 0 \quad \text{at} \quad x = a. \tag{10}$$

The top and bottom faces are insulated. The mould is cooled by removing uniformly a given amount of heat per unit time from the left- and right-hand sides. The boundary conditions on temperature are thus

$$\frac{\partial T}{\partial y} = 0 \quad \text{at} \quad y = 0, b$$

$$\frac{\partial T}{\partial x} = 0 \quad \text{at} \quad x = a$$

$$-k\frac{\partial T}{\partial x} = -Q \quad \text{at} \quad x = 0. \tag{11}$$

We assume that no solute is lost through the walls, and this is ensured if the normal gradient of c_m is prescribed to be zero at the wall and the line of symmetry

$$\frac{\partial c_m}{\partial x} = 0 \quad \text{at} \quad x = 0, a$$

$$\frac{\partial c_m}{\partial y} = 0 \quad \text{at} \quad y = 0, b. \tag{12}$$

Initially the alloy in the mould is assumed to be at rest, to be isothermal and of uniform composition, i.e.

$$\mathbf{u} = 0, \; T = T_i, \; c_l = c_i, \; \chi = 1 \quad \text{at} \quad t = 0 \tag{13}$$

where T_i is the initial temperature and c_i the initial composition.

The seven equations (1)–(9), together with boundary conditions (10)–(12) and the initial conditions (13), now completely specify the seven unknowns $\mathbf{u}$, p, T, c_m, c_l, c_s and χ. The methods used for solving the system are described in the next section.

3. NUMERICAL METHOD

A computer program that solves the equations given in the previous section in a two-dimensional rectangular domain has been developed. The computations are time dependent, and the solidification process is simulated from completely molten to completely solid. The equations have been discretized using a finite volume approach.

As is often done in phase change computations [3, 7] care has been taken to formulate equations that are valid throughout the domain, in both solid, mushy and liquid regions. It is then possible to use one simple net when discretizing the equations and, provided that the discretizations are done in a properly conservative manner, all continuity conditions at interfaces between solid and mush, and mush and liquid, are satisfied automatically.

In choosing the scheme for time discretization, it was observed that all equations except the phase diagram relation (8) allow a simple explicit time stepping. Equation (8) however algebraically couples two of the unknowns at the new time level in an unclear manner, in fact making the mathematical character of the entire system obscure. Therefore, it was decided to

replace equation (8) by the following seemingly artificial relation:

$$\frac{\partial \chi}{\partial t} = \frac{1}{\varepsilon}(T - T_L(c_l)). \tag{14}$$

Here T_L is the liquidus temperature as defined in the second equality of equation (8). This equation now allows a simple way of determining the melt fraction χ at the new time level: the right-hand side is evaluated using available values for temperature and composition, and the new melt fraction is readily obtained from the discretized left-hand side. If χ tends to increase beyond 1 or decrease below 0, the new value of χ is taken to be 1 or 0, respectively. This means that T is then allowed to differ from T_L, which of course is quite correct in the solid ($\chi = 0$) or liquid ($\chi = 1$) region.

The numerical parameter ε should be chosen small, so that any deviation of T from T_L is magnified and results in a rapid melting or freezing that restores T to T_L. A simple estimate shows that the error in equation (8) should be proportional to ε, and this is also confirmed numerically. By choosing a small enough value of ε, equation (8) can thus be satisfied to any desired degree of accuracy. The actual error is easily monitored in the computations by comparing T and T_L in the mush.

It should be pointed out that equation (14) may be seen as a crude way of allowing for a non-equilibrium phase transition with undercooling taking place. We have not attempted to give a physical interpretation of ε, nor to establish a numerical value that would describe undercooling, so ε should be regarded as a completely numerical parameter. However, it is reassuring that this numerical technique of using equation (14) instead of equation (8) mimics, qualitatively at least, a reasonable physical phenomenon.

The solution of the entire system, equations (1)–(7), (9) and (14), proceeds as follows: given temperature and composition at the previous time level, the new melt fraction is obtained explicitly from equation (14). From the new melt fraction value, the amount of released latent heat of fusion in the heat equation (5) and solute rejected from the solid in the composition equations (6), (7) and (9), are computed and temperature and concentrations may be obtained at the new time level. Using the new temperature, composition and melt fraction, a pressure and velocity field at the new time level is obtained from equations (1) and (4). All unknowns have then been computed at the new time level, and the procedure may be repeated.

Second-order accurate discretizations of spatial derivatives were used throughout. The velocity field is solved from equations (1) and (4) using the well-known pressure correction method [11, 12]. The non-linear convective term in equation (1) is discretized in a special manner to allow a reasonably large time step and to suppress non-physical oscillations in the solution [13]. In the heat equation (5) the diffusive term is treated implicitly, also to avoid a severe limitation of the time step size. Due to the very small value of mass diffusivity it is important to use a method that is stable for zero mass diffusivity when solving the concentrations from equations (6), (7) and (9). This is achieved by using an upwind discretization of the convective term in equation (7), as in the discretization of equation (1) [13].

The overall stability of the entire scheme is governed by a Courant number $Co = v_{max}\, dt/dy$, v_{max} being the maximal velocity in the domain and dy the spatial step size. Empirically it was found that Co should not exceed approximately 0.7, which gives a limit of the magnitude of the time step dt.

In the discussion of equation (14) above it was said that ε should be taken as small as possible. The minimal allowable value of ε is determined by the stability of the explicit solution of equation (14), giving ε proportional to dt. This is in fact sufficient: since the time step is governed by the rapid convection in the liquid region, dt is quite small. The allowable values of ε will typically give an error in satisfying equation (8) in the mush of less than 0.15% of the typical temperature variation over the mush.

The difference between the present method and that used by Bennon and Incropera [7], and Beckermann and Viskanta [8], is mainly that equation (14) is used instead of equation (8) here, which allows the system to be advanced to a new time level explicitly. Bennon and Incropera, and Beckermann and Viskanta, used a completely implicit method, where temperature, melt fraction, etc. at the new time level were obtained simultaneously as solutions to a non-linear system of equations. Their treatment allows larger time steps than the explicit method, but each step is more costly and it is not clear at present which of the two methods is the most economical.

Another point is that Bennon and Incropera [7], and Beckermann and Viskanta [8] did not present results for the mixture composition. For the melt fraction, only the boundaries between solid and mush, and mush and liquid were presented. Since we are interested in the development of macrosegregation, the distribution of mixture composition and the evolution of the melt fraction are of prime importance, and are presented in the next section.

4. RESULTS

The program described above was used to compute the solidification of an iron–carbon alloy in a small mould. Values of the relevant physical parameters are given in Table 1. Initially the melt was assumed to be at rest, and at a uniform temperature and composition. At time zero the cooling of the side walls began by removing uniformly a given power. The top and bottom faces were insulated.

The mould was taken to be rectangular with 10 cm height and 20 cm width, i.e. $a = b = 10$ cm. The initial composition was chosen to be $c_i = 1$ wt%. The initial temperature was $T_i = 1463$°C, i.e. 5°C above the melt-

ing temperature at 1 wt% carbon. In the following temperatures will be referred to the melting temperature of pure iron, so that the initial temperature is -73°C, and the melting temperature at 1 wt% carbon is -78°C. Heat was removed from the side walls at a rate of $Q = 60$ kW m^{-2}. The time for removing the latent heat of fusion is thus 3146 s or approximately 52 min. Since the specific heat must also be removed, the solidification will take at least this long.

The qualitative behaviour of the convection in the liquid region is determined by the values of the Prandtl number $Pr = \mu C/k$, and the Rayleigh number $Ra = g\alpha'\Delta T b^3/(k\mu/\rho_0^2 C)$. The appropriate temperature ΔT is the temperature variation over the melt region, i.e. the difference between the initial temperature and that at the mush–liquid interface, i.e. 5°C. The numbers in Table 1 then give the values $Ra = 3.59 \times 10^6$ and $Pr = 0.1742$. The flow is thus expected to be rapid, but certainly laminar.

Figure 2 shows velocity vectors and lines of constant melt fraction at different instants. At $t = 200$ s, Fig. 2(a), a mush occupying about one third of the mould half width has appeared on the left-hand side. Cooled heavy liquid falls down along the mush surface and fills the interior of the mould from the bottom. The typical velocity in the boundary layer is a little less than 1 cm s^{-1}. As shown in Fig. 3(a), a vertical temperature gradient has been set up in the interior (as is common in thermal convection in cavities [14]). Since the composition is virtually unchanged in the completely molten region, the interface between mushy and liquid regions is kept at the melting temperature -78°C corresponding to 1 wt% carbon (in the following temperatures will be referred to the freezing temperature of pure iron). The effect of the convection in the completely molten region is thus to cool the entire molten region towards -78°C, and to eliminate horizontal temperature variations outside the boundary layer on the surface of the mushy zone. At $t = 200$ s, the liquid metal in the completely molten region has already cooled from -73°C to around -77°C.

At $t = 400$ s, Figs. 2(b) and 3(b), the mush occupies approximately two thirds of the mould half width. The temperature in the molten part has come quite close (within 0.2°C) to the melting temperature -78°C. Since the driving temperature difference is now rather small, the strength of the convection has decreased considerably. The composition is still virtually unchanged in the molten part. As the temperature of the melt decreases further, it will become even more isothermal, and the entire molten region will reach its freezing temperature almost simultaneously. A thin mush will then rapidly grow across the entire mould. This occurs at around 500 s after the start of cooling.

At $t = 800$ s, Figs. 2(c) and 3(c), the mush fills the mould. It is very thin towards the centre. Since velocities are very much smaller in the mush than in the molten region, the velocity vectors have been magnified in Figs. 2(c), 2(d) and 2(e). There is a slow clockwise convection (the opposite sense as compared to the earlier convection in the liquid region) through the mush. This convection is caused by enrichment of the melt, which makes it lighter, due to the exclusion of carbon from the growing solid dendrites. A typical velocity is now 0.01 mm s^{-1}, so that the fluid moves approximately 1 cm in 1000 s, the order of magnitude of the time available before the mould is more or less solid. Thus we should expect a rather moderate macrosegregation in the finished ingot with a composition deviating appreciably from 1% in regions 1–2 cm thick at the top and bottom.

At $t = 1800$ s $= 0.5$ h, the melt fraction increases approximately linearly from 0.16 at the left wall to 0.86 at the centreline, Figs. 2(d) and 3(d). The mesh is notably thinner in a region of about 2 cm depth below the top, and slightly thicker in a corresponding area above the bottom. The clockwise convective cells is weaker and is displaced to the right (centre). There is virtually no convection where the melt fraction is less than 0.4. The presence of macrosegregation is now evident in the shapes of the isotherms and the isolines for melt fraction: if no segregation had taken place, melt fraction would be a function of temperature, and so the two families of curves would have the same shapes, but this is not the case.

At $t = 3600$ s $= 1$ h, Figs. 2(e) and 3(e), the melt fraction is less than 0.2 in most of the mould. The largest fraction of melt is present in the top centre. There is no appreciable convection due to the low permeability in a mush this dense.

In Fig. 3, the isotherms have been plotted along with those for the local liquidus temperature, which is obtained from the melt composition according to equation (8). The levels of the liquidus isotherms are chosen as the levels appearing in the mush, i.e. -80°C, -90°C, ..., -180°C. In Figs. 3(a)–(d) the isotherms corresponding to the temperature and the liquidus temperature coincide. In the mushy region, the temperature should of course always equal the liquidus temperature, and the degree to which it does is a test of the accuracy of the numerical scheme. Only in the lower left corner of Fig. 3(e) is there a visible difference, where the temperature isotherm is practically vertical, but the liquidus isotherm bends sharply to the left. Comparison with Fig. 2(e) shows however that this lower left corner is solid, so that the liquidus temperature should be higher than the temperature, which is precisely what Fig. 3(e) shows.

Figure 4 shows isolines of the mixture composition, see equation (6), at different times. If no macrosegregation occurs at all this composition will remain a constant equal to the initial value of 1%, even if the solute is very unevenly distributed between the solid and liquid phases in the mush. When the ingot is completely solidified, c_m of course equals c_s, and will thus show the final distribution of carbon in the finished ingot.

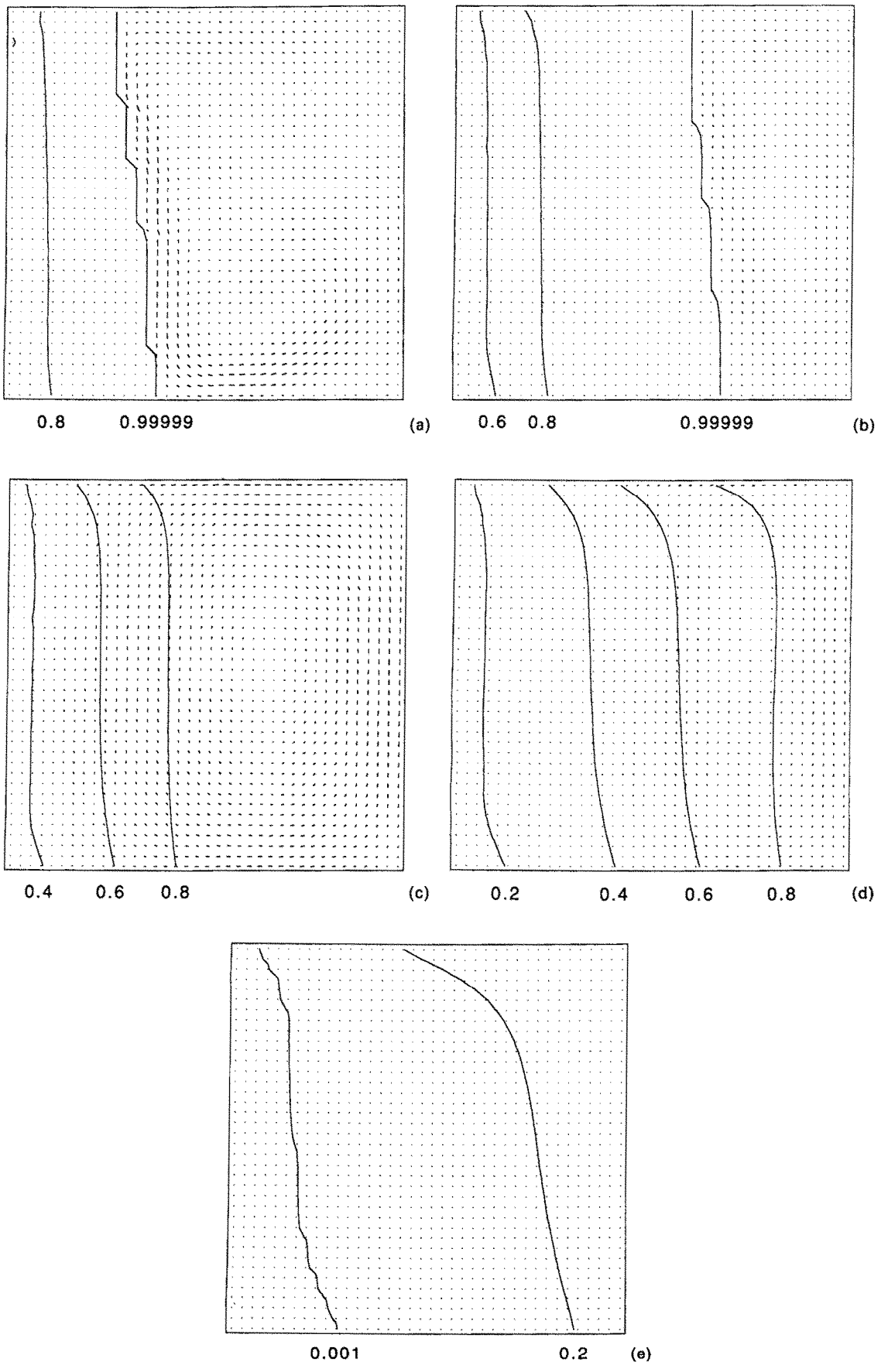

FIG. 2. Velocity vectors and constant melt fraction contours at different times after the start of cooling: (a) $t = 200$ s; (b) $t = 400$ s; (c) $t = 800$ s; (d) $t = 1800$ s; (e) $t = 3600$ s. The melt fraction levels are $\chi = 0.001$, 0.2, 0.4, 0.6, 0.8, 0.99999. In (a) and (b) a velocity vector length equal to the mesh spacing corresponds to a velocity of 1 cm s^{-1}. In (c), (d) and (e) it corresponds to 0.05 mm s^{-1}.

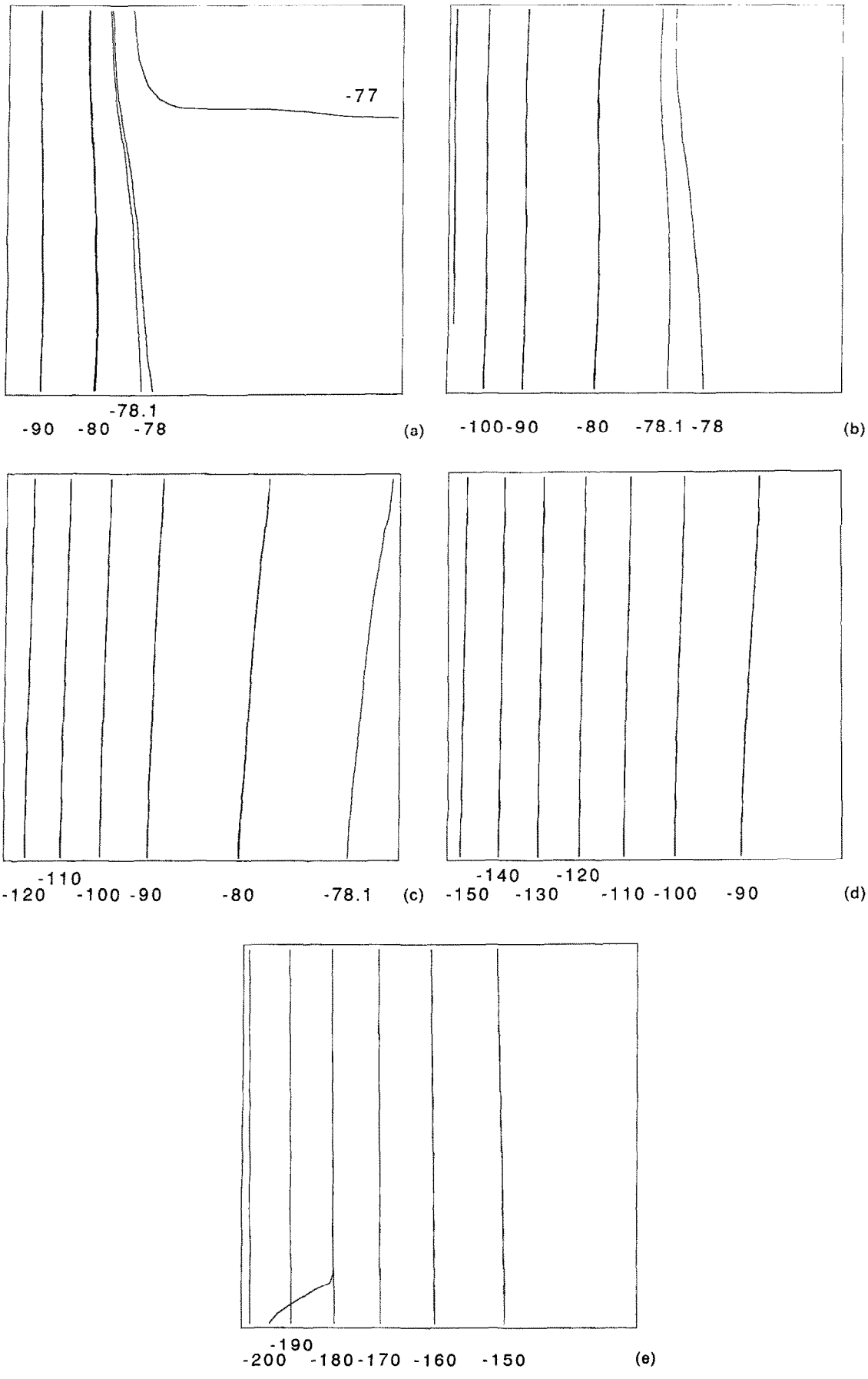

FIG. 3. Isotherms of the temperature and the liquidus temperature: (a) $t = 200$ s; (b) $t = 400$ s; (c) $t = 800$ s; (d) $t = 1800$ s; (e) $t = 3600$ s. The levels are -75, -77, -78, -78.1, -80, -90, $-100, \ldots, -200$°C for temperature, and -80, -90, $-100, \ldots, -180$°C for liquidus temperature.

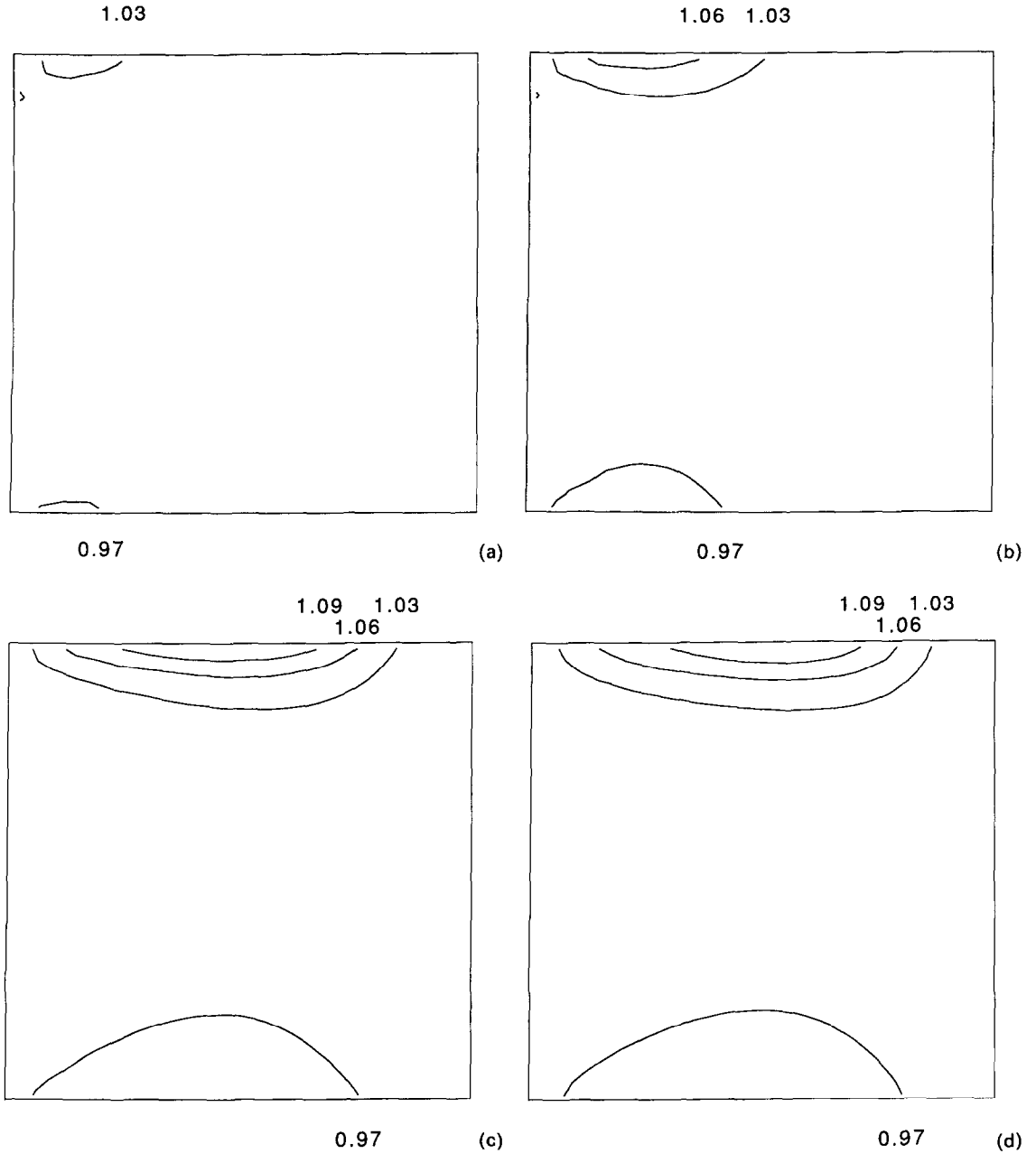

FIG. 4. Contours of constant mixture composition c_m at different times: (a) $t = 400$ s; (b) $t = 800$ s; (c) $t = 1800$ s; (d) $t = 6000$ s. The composition levels are 0.97, 1.03, 1.06 and 1.09%.

Early, at $t = 400$ s, Fig. 4(a), only a slight enrichment and depletion at the top and bottom left respectively, is seen. Later at $t = 800$ s, the pattern becomes more pronounced. It evolves further and is more or less stationary at $t = 1800$ s. The final plot, Fig. 4(d), is at $t = 6000$ s, when the mould is completely solid. The plot of c_m in Fig. 4(d) thus shows the final distribution of carbon. A moderate segregation is shown there, with an enrichment of up to 10% of the original composition along a 1–2 cm wide band along the top. A corresponding depletion is visible along the lower wall.

The general behaviour that is predicted here agrees with experience from real castings. There should certainly be an enrichment of solute at the top and depletion at the bottom. The magnitude of the final segregation is reasonable. One feature that differs somewhat from experience is the prediction of a very thin mush appearing fairly early in the solidification process, extending over the entire mould. This is seen

in Figs. 2(b) and (c). In Fig. 2(b) a region where solid fraction is below a few per cent extends roughly from one third to two thirds of the half width, measured from the left wall. In Fig. 2(c), the right half of the mould half width is occupied by a very thin mush, with solid fraction less than a few per cent. However, it is probably not physically reasonable to have a mush this thin extending over such large regions. Probably the undercooling that indeed is present in these regions, should result in the formation of free equiaxed crystals instead of a mush attached to the wall. Also some undercooling would be required to advance the front of the mush into liquid. This could be taken into account by prescribing a kinetic law for the front of the mushy zone, relating the velocity of the front to the undercooling [4, 15]. This will be investigated in a future study.

The numerical technique was found to work well. The usual problems with computing a flow characterized by a fairly high Rayleigh number, as well as the difficulties arising from the simulation of the solidification itself could be surmounted.

As was discussed above, the phase diagram equation (8) is only satisfied approximately, by the use of equation (14) instead of equation (8). The validity of this is easily checked by comparing T and $T_L(c_l)$ in the mush. Isotherms of both T and $T_l(c_l)$ are drawn in Fig. 3, and they are hardly distinguishable. The magnitude of a typical error may be extracted from the results in Fig. 3(d), at $t = 1800$ s. Comparing T and $T_L(c_l)$ along the mid height $y = 5$ cm, shows that the maximal error is less than 0.1 C. This should be related to the temperature difference over the mould which is 68 C in Fig. 3(d), i.e. a relative error below 0.15%, which is certainly permissible.

5. CONCLUSIONS

A numerical method for simulating a freezing alloy was presented. It has been applied to the solidification of an iron–carbon alloy in a rectangular mould cooled from the sides.

When the cooling starts, a mush begins to grow from the cooled wall. The liquid region is cooled to the temperature of the mush–liquid interface, i.e. the freezing temperature at the undisturbed initial composition. The thermal convection in the fluid region that is immediately set up, causes the fluid to become more and more isothermal. The composition is practically unchanged in the liquid region.

The flow in the mushy region is dominated by solutal instead of thermal convection. Due to the low permeability of the mush, this is roughly 1000 times slower. It is caused by enrichment of solute in the interdendritic liquid as the mush freezes, which makes the liquid buoyant. The resulting motion is thus in the opposite sense compared to the thermal convection. It is this slow motion that causes macrosegregation. The major effect of the much more rapid convection in the molten region is to keep the liquid mixed and isothermal, but it does not cause segregation since the composition variation is very small in the liquid region. In the mush, the exclusion of solute from the growing solid dendrites causes considerable composition gradients in the liquid. Convection will then result in a net transport of solution, i.e. macrosegregation.

The simulation was pursued until the mould was completely solid. A depletion of solute is seen near the bottom and an enrichment at the top.

The numerics were found to perform well, giving smooth results for both the solid composition and the melt fraction. The error in satisfying the phase diagram relations were found to be permissibly small.

One discrepancy with the experience from real casts that was observed, was the appearance of a thin mush extending over a large part of the mould. In reality this does probably not occur. A more accurate modelling of the interface between the mushy and liquid regions would include an undercooling of the dendrite tips at the interface between the mushy and the liquid regions. This could be described by a kinetic law relating the growth velocity of the dendrite tips at the interface between the mushy and liquid regions to the local undercooling. In a future study the result of including such a model in the code, as well as detailed comparisons with experimental results, will be reported.

Acknowledgement—I am grateful to Professor H. Fredriksson for many discussions that have been instrumental for the completion of this work.

REFERENCES

1. M. C. Flemings and G. E. Nereo, Macrosegregation: part I, *Trans. TMS–AIME* **239,** 1449–1461 (1967).
2. M. C. Flemings, *Solidification Processing*. McGraw-Hill, New York (1974).
3. V. R. Voller and C. Prakash, A fixed grid numerical modelling methodology for convection–diffusion mushy region phase-change problems, *Int. J. Heat Mass Transfer* **30,** 1709–1719 (1987).
4. S. C. Flood and J. D. Hunt, A model of casting, *Appl. Scient. Res.* **44,** 27–42 (1987).
5. R. N. Hills, D. E. Loper and P. H. Roberts, A thermodynamically consistent model of a mushy zone, *Q. J. Mech. Appl. Math* **36,** 505 (1983).
6. M. G. Worster, Solidification of an alloy from a cooled boundary, *J. Fluid Mech.* **167,** 481–501 (1986).
7. W. D. Bennon and F. P. Incropera, A continuum model for momentum, heat and species transport in binary solid–liquid phase change systems—II. Application to solidification in a rectangular cavity, *Int. J. Heat Mass Transfer* **30,** 2171–2187 (1987).
8. C. Beckermann and R. Viskanta, Double-diffusive convection during dendritic solidification of a binary mixture, *PhysicoChem. Hydrodyn.* **10,** 195–213 (1988).
9. A. Olsson, Ph.D. Thesis, Department of Casting of Metals, Royal Institute of Technology, Stockholm, Sweden (1980).
10. R. West, On the permeability of the two-phase zone during solidification of alloys, *Metall. Trans. A* **16,** 693 (1985).
11. C. A. J. Fletcher, *Computational Fluid Mechanics*. Springer, Berlin (1988).

12. J. van Kan, A second order accurate pressure-correction scheme for viscous incompressible flow, *SIAM J. Sci. Stat. Comput.* **7**, 870 (1986).
13. R. W. Davis and E. F. Moore, A numerical study of vortex shedding from rectangles, *J. Fluid Mech.* **116**, 475–506 (1982).
14. J. Patterson and J. Imberger, Unsteady natural convection in a rectangular cavity, *J. Fluid Mech.* **100**, 65–86 (1980).
15. R. C. Kerr, A. W. Woods, M. G. Worster and H. E. Huppert, Disequilibrium and macrosegregation during solidification of a binary melt, *Nature* **340**(6232), 357–362 (1989).

CALCUL DE LA MACROSEGREGATION DANS UN FORGEAGE FER–CARBONE

Résumé—On présente une méthode numérique de calcul de macroségrégation dans un alliage en solidification. La formulation porte sur la loi de conservation de la masse, de la quantité de mouvement, de la chaleur et du soluté et sur les relations thermodynamiques qui gouvernent le changement de phase. Le mécanisme complet, fonction du temps, est simulé jusqu'à la solidification complète. La méthode est appliquée au cas d'un système fer–carbone qui se solidifie dans un nombre rectangulaire bidimensionnel, refroidi par les bords. On calcule la convection thermique et solutale pendant la solidification. L'évolution de la fraction fondue dans le moule est décrite ainsi que la distribution finale de carbone après solidification.

BERECHNUNG VON MAKROSKOPISCHEN ENTMISCHUNGSERSCHEINUNGEN IN EISEN–KOHLENSTOFF-SCHMELZEN

Zusammenfassung—Es wird ein numerisches Berechnungsverfahren für die makroskopische Entmischung in einer erstarrenden Schmelze vorgestellt. Das Modell beruht ausschließlich auf den grundlegenden Erhaltungssätzen für Masse, Impuls, Wärme und Stoff, sowie die thermodynamischen Beziehungen für den Phasenwechsel. Der gesamte zeitlich veränderliche Vorgang wird simuliert—bis hin zur vollständigen Verfestigung. Das Verfahren wird auf den Fall eines Eisen–Kohlenstoff-Systems angewandt, das sich in einer zweidimensionalen rechtwinkligen, seitlich gekühlten Form verfestigt. Die temperatur- und konzentrationsgetriebene Konvektion während der Verfestigung wird berechnet. Die zeitliche Entwicklung des Anteils der Schmelze in der Form und die Verteilung des Kohlenstoffs nach der Verfestigung wird dargestellt.

РАСЧЕТ МАКРОСКОПИЧЕСКОЙ СЕГРЕГАЦИИ В СПЛАВЕ ЖЕЛЕЗО – УГОЛЬ

Аннотация—Предложен численный метод расчета макроскопической сегрегации в затвердевающем сплаве. Формулировка задачи основана на фундаментальных законах сохранения массы, импульса, тепла и растворенного вещества, а также на термодинамических зависимостях, определяющих фазовый переход. Моделируется нестационарный процесс до полного затвердевания. Метод применяется к системе железо – уголь, затвердевающей в двумерной прямоугольной прессформе, охлаждаемой с обеих сторон. Рассчитываются конвективный перенос тепла и растворенного вещества при затвердевании. Описываются эволюция доли расплава в прессформе и окончательное распределение угля после затвердевания.